

# Comprehensive Analysis of Curcumin Zinc Oxide Nanoparticles, Synthesis, Characterization, and Cytogenotoxic Profiling

Alia Saif, Muhammad Ovais Omer,\* Adeel Sattar, Yasin Tipu, Hanan M. Alharbi, Uzma Saher, and Tanzeela Awan



Cite This: *ACS Omega* 2024, 9, 28186–28193



Read Online

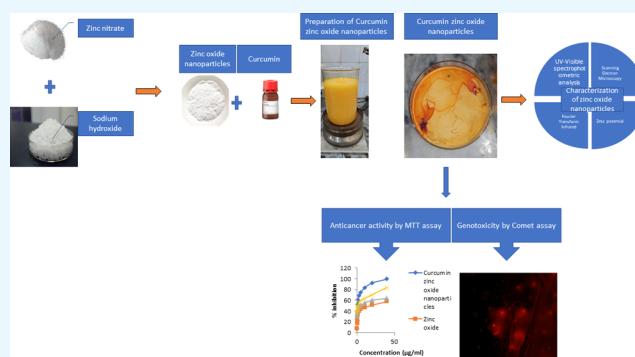
ACCESS |

Metrics & More

Article Recommendations

Supporting Information

**ABSTRACT:** Curcumin from turmeric (*Curcuma longa*) has traditionally been used due to its pharmacological properties, such as anticancer, anti-inflammatory, cholesterol-lowering, and antioxidant activities, but has had limitations in use due to low bioavailability. Nanoparticles have protuberant efficacies to diagnose or cure a variety of diseases, including tumors, by fine-tuning their size, structure, and physicochemical characteristics. This study aims to develop a new dosage form of curcumin nanoparticles with zinc oxide to enhance its therapeutic efficacy against cancer and cause no damage to genetics. Curcumin zinc oxide nanoparticles were prepared and characterized by using a Zeta sizer, ultraviolet (UV)-spectrophotometer, scanning electron microscope (SEM), and Fourier transform infrared (FTIR) spectroscopy. Different concentrations range from 40 to 0.078  $\mu\text{g}/\text{mL}$ , and these nanoparticles were evaluated for their anticancer activity by colorimetric analysis (MTT assay) on normal (Vero) and cancerous cell lines (MCF-7) and genotoxicity by the comet assay. The spherical-shaped curcumin zinc oxide nanoparticles of 189 nm size were prepared with characteristic functional groups. The selectivity index of curcumin zinc oxide nanoparticles, calculated from  $\text{IC}_{50}$  values, is  $4.60 > 2.0$ , showing anticancer potential comparable to tamoxifen. The genetic damage index of the highest concentration (40  $\mu\text{g}/\text{mL}$ ) of curcumin zinc oxide nanoparticles was 0.08, with a percent fragmentation of 8%. The results suggest that nanoparticles of curcumin zinc oxide produced better anticancer effects and did not cause any significant damage to the DNA. Consequently, further research is required to ensure the development of a safe and quality dosage form of nanoparticles for proper utilization.



## 1. INTRODUCTION

Cancer is daunting in the breadth and scope of its diversity, spanning genetics, cell and tissue biology, pathology, and response to therapy. The most prevalent form of malignant tumor is breast cancer, causing early death in women worldwide.<sup>1</sup> Typical issues associated with breast tumors include their resistance to conventional therapeutic protocols and the risk of recurrence, even after 10 years of treatment. To lessen the likelihood of breast cancer, a woman must take particular precautions, such as breast cancer screening, and recognize breast cancer risk factors, such as family history, menopause, etc. Although some risk factors can be managed, others are more challenging.<sup>2</sup>

Tamoxifen (TAM), a selective modulator of estrogen receptor (ER) in breast tissues, is commonly employed as an adjuvant treatment therapy in premenopausal and postmenopausal patients suffering from breast cancer. It counteracts the physiological effect of estrogen that is circulating in the blood, thus preventing its effect on the growth of tumors, which in turn controls the proliferative effects in tissues like the endometrial lining and bones.<sup>3</sup> However, plants have been

identified as the major source of a variety of drugs by the World Health Organization (WHO) as they are abundant in therapeutic components. Numerous bioactive compounds are produced by plants as part of their natural defense mechanism.<sup>4</sup> Medicinal plants have a high concentration of phytochemicals, which can be structurally improved and converted to novel medications.<sup>5</sup>

Curcumin, a therapeutically active ingredient obtained from the rhizome of Turmeric (*Curcuma longa*; *Zingiberaceae*), is a crystalline bright orange chemical that is insoluble in acidic or neutral pH, i.e., water, but soluble in strong acidic solvents and polar and nonpolar organic solvents.<sup>6</sup> Its chemical formula is  $\text{C}_{21}\text{H}_{20}\text{O}_6$  with a melting point of 183 °C and molecular weight of 368.38 Da. The majority of curcuminoid chemical research

Received: February 15, 2024

Revised: June 7, 2024

Accepted: June 10, 2024

Published: June 24, 2024



has been done on experimental lab animals, with only a few trials on human subjects.<sup>7</sup> Curcumin has been demonstrated to be safe for human use in clinical tests, even at high doses, although its medical utility is limited since it has limited bioavailability.<sup>8</sup> It has pleiotropic actions on a wide range of molecular targets, including antioxidative, anti-inflammatory, chemo-preventive, chemotherapeutic, and antidiabetic activities, all with minimal adverse effects.<sup>9</sup> The novel approach to achieving efficient delivery of medicinal compounds to the site of action is by formulating nanosized particles or nanoparticles (NPs) of drug molecules.

Nanoparticle biosynthesis has been presented as a cost-effective and environmentally friendly alternative to physical or chemical processes. Plant-mediated nanoparticle synthesis is a green chemistry technique that combines nanotechnology and plants.<sup>10</sup> The most common approach for making magnetic nanoparticles is to use physical and chemical methods. The physical ball milling process is classified into two categories, i.e., regular ball milling and high-energy ball milling.<sup>11</sup> Conventional methods have been employed over the years, but studies have shown that the green method is efficient for the synthesis of NPs as it has fewer risks of failure, is less expensive, easier to characterize, and contributes more to the upkeep of the pharmaceutical sector.<sup>12</sup>

Various medicinal plants have bioactive molecules that exhibit potent anticancer effects that can stop the growth of tumors and cause cancer cells to undergo apoptosis. Nevertheless, it is critical to take into account the possibility that some medicinal plant constituents may also have genotoxic effects, potentially harming the DNA of healthy cells. A careful assessment of the genotoxic potential of medicinal plant components is required to establish a balance between their therapeutic and anticancer benefits while minimizing any potential genotoxic issues. Keeping in view the aforementioned realities, this research aims to formulate and characterize curcumin zinc oxide nanoparticles and also evaluate these NPs to provide insight into their anticancer and genotoxic effects. The purpose of this study is to develop safer and more efficient therapeutic techniques in cancer treatment.

## 2. MATERIALS AND METHODS

**2.1. Chemicals and Reagents.** All experimental chemicals were of analytical grade and purchased from Sigma-Aldrich, Germany. Curcumin powder, zinc nitrate  $Zn(NO_3)_2$ , and cetyltrimethylammonium chloride (CTAC) were purchased to prepare the nanoparticles. Cell culture media, ethidium bromide, low melting point agarose (LMPA), normal melting point agarose (NMPA), lymphocyte separating media (Histopaque), Trizma base, triton X-100, disodium ethylene diamine tetraethylene amine (Disodium EDTA), phosphate buffer tablets, and dimethyl sulfoxide (DMSO) were purchased for toxicological tests.

**2.2. Preparation of Curcumin with Zinc Oxide Nanoparticles.** Zinc nitrate and sodium hydroxide solutions were prepared separately with distilled water in a 1:2 molar ratio. The  $Zn^{2+}$  solution was mixed with a cetyltrimethylammonium chloride (CTAC) solution, and then the NaOH solution was added dropwise. The mixture was centrifuged (HERMLE Z 300 K—Centrifuge machine), washed thrice with water and once with ethanol, and dried in an oven overnight at 60 °C. Curcumin was dissolved in acetone at a concentration of 2 mg/mL and ZnO nanoparticles (ZNPs) at a concentration of 10 mg/mL. The curcumin solution was then

mixed with ZnO solution. To finish the grafting/surface adsorption of curcumin to ZnO and formulate the ZnO–curcumin nanocomposite (ZNP–C), this mixture was agitated for 24 h using a magnetic stirrer (Thermo-Fischer Scientific). The resulting suspension was centrifuged at 6000 rpm, rinsed 3 times with distilled water, and then vacuum-dried (Thermo-Fischer Scientific).<sup>13</sup>

**2.3. Characterization of Nanoparticles.** **2.3.1.  $\zeta$ -Potential.** The Malvern Zetasizer analyzes the charge and size of drug nanoparticles, particularly focusing on determining the  $\zeta$ -potential to assess interactions with negatively charged cells. The sample was diluted with water and positioned in the electrophoretic chamber, where an electric field of 15.2 V/cm was applied.<sup>14</sup>

**2.3.2. UV-Vis Spectra Analysis.** Ultraviolet–visible (UV–vis) spectrophotometer analysis was used to track the generation and stability of decreased nanoparticles in colloidal solution. For analyzing various metal oxides in the size range of 2 to 100 nm with BMS, UV-1502 spectrophotometer, light wavelengths in the 300–800 nm range are commonly utilized.<sup>15</sup>

**2.3.3. Scanning Electron Microscopy (SEM).** Scanning electron microscopy of curcumin zinc oxide nanoparticles was performed with an SEM model number JEOL JSM 6480 LV. This technique was employed to see the morphology of nanoparticles. Curcumin nanoparticles were sterilized through ultraviolet light in laminar airflow for 30 min. With adhesive tape, the sterilized nanoparticles were carefully placed on SEM stubs and were scanned using magnifications ranging from  $\times 15,000$  to  $\times 35,000$ .<sup>16</sup>

**2.3.4. Fourier Transform Infrared Spectroscopy (FTIR).** ATR-FTIR spectroscopy is a common technique used for analyses, as it provides valuable insights into the chemical composition and structure of the samples. In this study, FTIR spectroscopy, specifically attenuated total reflectance Fourier transform infrared (ATR-FTIR) spectroscopy, was utilized as an analytical approach to identify the functional groups present in curcumin zinc oxide nanoparticles. The nanoparticles were analyzed using an FTIR spectrometer in the wavenumber range between 4000 and 400  $cm^{-1}$ . The FTIR measurements of curcumin zinc oxide nanoparticles were conducted using a BRUKER  $\alpha$  model<sup>17</sup>

**2.4. Evaluation of Anticancer Activity of Drug: Cell Viability Analysis (MTT Assay).** In vitro cytotoxicity analysis was performed by performing an MTT assay on Vero (normal) and MCF-7 (cancerous) cell lines. NADPH-dependent oxidoreductase enzymes under defined conditions reflect the number of viable cells present, resulting in a reduction of tetrazolium dye to insoluble formazan showing a purple color.<sup>14</sup> Cells were first seeded in the 96 well plates and incubated for 24 h at 37 °C. With the help of phosphate-buffered saline (PBS), the cells were washed and then inoculated with or without the final drug concentrations. The medium was aspirated after 48–72 h of incubation. Plates were incubated (Thermo-Fischer Scientific – CO<sub>2</sub> Incubator) for 4 h at 37 °C after the addition of MTT solution in PBS, in each well under dark conditions. After incubation, 100  $\mu$ L of dimethyl sulfoxide (DMSO) was added to each well and gently shaken for 15 min to solubilize formazan dye. Multiskan Microplate Photometer (Thermo-Fischer Scientific) was used to check absorbance at 540 nm.

**2.4.1. Selectivity Index (SI).** The comparison of IC<sub>50</sub>, obtained from the data of absorbance values of a pure

compound and their combinations on both cancerous and normal cell lines, gave the value of selectivity index, which explained the differential activity of combinations and pure compounds. The anticancer potential was determined by finding the selectivity index (SI) of pure compounds and then in combination.

$$SI = \frac{IC_{50} \text{ on cell lines}}{IC_{50} \text{ on cancerous cell lines}}$$

**2.5. Evaluation of Genotoxicity of the Drug: (Comet Assay).** The comet assay is a type of single-cell gel electrophoresis (SCGE) used to study the genotoxicity of different concentrations of nanoparticles.<sup>18</sup> For the in vitro comet assay, lymphocytes from fresh blood samples obtained from Medical Center UVAS, Lahore, were separated. Dimethyl sulfoxide (20%) and normal saline were used as positive and negative controls, respectively. Cavity slides were immersed in methanol, burned over a blue flame, and then dipped in hot, normal melting agarose. Lymphocytes were exposed to different concentrations of the test samples. Slides filled with lymphocyte suspension combined with low melting agarose were exposed to a cooled lysing solution overnight and then exposed to an alkaline buffer solution with a pH greater than 13. The slides were then subjected to electrophoresis for 30 min at 300 mA and 24 V and then placed in neutralizing buffer at pH 7.5. The slides were then stained with Ethidium bromide. Comet tail lengths and variations in head diameter were measured using ImageJ software version 1.8.0, which was calibrated using a fluorescence microscope. The damage index was determined using the formula given below

$$\begin{aligned} \text{damage index} = & (\text{number of cells in class 1}) \\ & + (2 \times \text{number of cells in class 2}) \\ & + (3 \times \text{number of cells in class 3}) \end{aligned}$$

**2.6. Statistical Analysis.** The raw data obtained for all experiments were analyzed by IBM SPSS (Statistical Package for the Social Sciences version 20, Inc., Chicago IL) and expressed in terms of means  $\pm$  SD, where the number of nanoparticles was at least three to five. The analysis of variance (ANOVA) along with POST HOC Duncan's test was applied to find statistical differences.

### 3. RESULTS

**3.1. Characterization.** After formulation, the nanoparticles were characterized by zeta sizer and spectral methods like UV–visible spectroscopy, FTIR spectroscopy, and SEM, as these are the traditional and effective methodologies for the determination of nanoparticle formation.

**3.1.1.  $\zeta$ -Potential of Curcumin Zinc Oxide Nanoparticles.** The particle size of curcumin zinc oxide nanoparticles was found to be 189 nm (Figure 1), with a polydispersity index of 0.003, representing its uniformity. Further, the zeta potential was found to be  $-36.4$  for curcumin zinc oxide nanoparticles (Figure 1). The particle distribution intensity (PDI) value of these nanoparticles was 0.003.<sup>19</sup>

**3.1.2. UV–Visible Spectra Analysis of Curcumin Zinc Oxide Nanoparticles.** The concentration and characterization of curcumin zinc oxide nanoparticles were confirmed by using UV spectrophotometry, which showed the maximum absorbance of the nanoparticle solution at a bend curve near 418 nm, which was a convenient region of the spectrum.

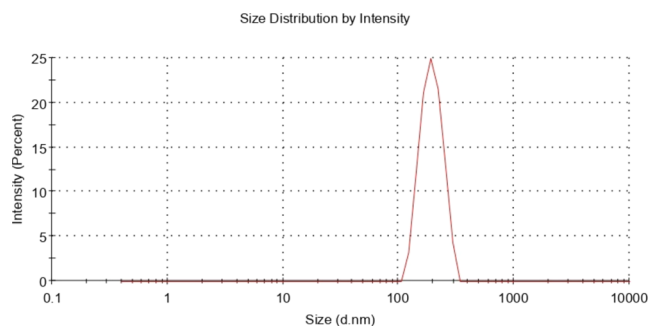


**Figure 1.** Size of nanoparticles by the  $\zeta$ -potential of curcumin zinc oxide nanoparticles: The size of curcumin zinc oxide nanoparticles was measured by Malvern zeta sizer and found to be 189 nm. A graphical representation is shown here; the  $x$ -axis represents the size in nm, and the  $y$ -axis shows the intensity of the particles in percentage.

**3.1.3. SEM Analysis of Curcumin Zinc Oxide Nanoparticles.** Upon SEM analysis, curcumin zinc oxide nanoparticles appeared to be spherical. Figure 2 shows the SEM images of curcumin zinc oxide nanoparticles.

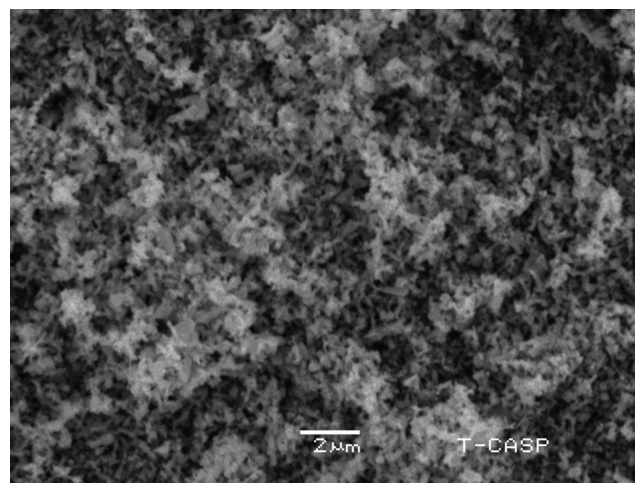


**Figure 2.** SEM analysis of curcumin zinc oxide nanoparticles: The scanning electron microscopy of curcumin zinc oxide nanoparticles was performed after sterilization of nanoparticles under UV light in laminar airflow. The image shows the spherical-shaped particles. A representative image is shown. The scale bar indicates an area of 2  $\mu\text{m}$ .

**3.1.4. FTIR Analysis of Curcumin Zinc Oxide Nanoparticles.** FTIR spectroscopy is a commonly used method to determine the functional groups of various organic compounds. In this study, FTIR spectroscopy was performed in the range 4000–400  $\text{cm}^{-1}$ . The FTIR spectrum showed the expected Zn–O stretching vibrations at 677  $\text{cm}^{-1}$ , as well as vibrations of metal oxides at 802, 833, and 881  $\text{cm}^{-1}$ . The benzoate *trans*-C–H vibration was observed at 962  $\text{cm}^{-1}$ . The peaks observed at 1197 and 3346  $\text{cm}^{-1}$  are likely due to O–H deformation of the NP surface and stretching from the moisture adsorbed on the NP surface, respectively. FTIR analysis of curcumin zinc oxide nanoparticles clearly showed the presence of characteristic absorption bands at 1627  $\text{cm}^{-1}$  due to C=C benzene stretching ring, at 1509  $\text{cm}^{-1}$  due to C=O stretching, at 1428  $\text{cm}^{-1}$  due to C–H bending, at 1280  $\text{cm}^{-1}$  due to C–O stretching, at 1025  $\text{cm}^{-1}$  due to C–O–C stretching vibration, and at 856  $\text{cm}^{-1}$  due to C–H aromatic



hydrogen. Figure 3 shows the graph of curcumin zinc oxide nanoparticles obtained by FTIR analysis.

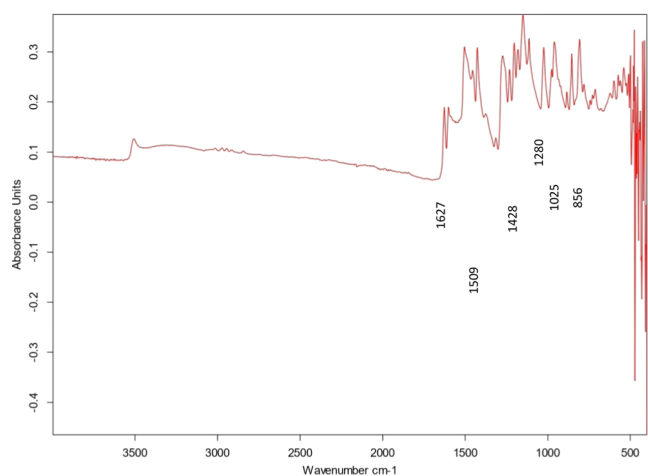


**Figure 3.** FTIR of curcumin zinc oxide nanoparticles: The FTIR analysis shows waves at various points due to the stretching of specific bonds and rings. A graphical representation has been shown here; the  $x$ -axis represents the wave numbers per centimeter, and the  $y$ -axis shows the absorbance units.

**3.2. Evaluation of the Anticancer Activity of the Drug, Cell Viability Analysis (MTT Analysis).** The anticancer and cytotoxic potential of curcumin zinc oxide nanoparticles was quantified on MCF-7 and Vero cell lines, respectively. Ten different concentrations of curcumin zinc oxide nanoparticles were incubated for 48 h with MCF-7 and Vero cell lines in a CO<sub>2</sub> incubator. The selectivity index was calculated by IC<sub>50</sub>. Tamoxifen was used as a standard.

The highest concentration (40  $\mu\text{g/mL}$ ) of the nanoparticles had a percentage inhibition of 99.75%, whereas the curcumin and zinc oxide showed a percentage inhibition of 64.00 and 57.98% against the MCF7 cell line, respectively, as shown in Figure 4A. However, Curcumin zinc oxide nanoparticles had a percentage inhibition against normal cells (Vero cells) at 78.50%, close to tamoxifen with 75.18% inhibition, as shown in Figure 4B. A statistical comparison of percentage inhibition

was made at each concentration, which suggests that the results are highly significant.

The selectivity index of curcumin zinc oxide nanoparticles showed comparable anticancer activity to tamoxifen and had low IC<sub>50</sub> values against MCF7 cell lines compared to curcumin and zinc oxide, as given in Table 1. The selectivity index of

**Table 1. IC<sub>50</sub> and Selectivity Index**

drug	IC <sub>50</sub>		selectivity index
	MCF7 cell line ( $\mu\text{g/mL}$ )	Vero cell line ( $\mu\text{g/mL}$ )	
curcumin zinc oxide nanoparticles	2.085	9.592	4.60
curcumin	11.459	23.201	2.02
zinc oxide	23.909	32.154	1.344
tamoxifen	2.377	13.523	5.68

curcumin is slightly more than 2, which shows that it has toxicity against cancer cells but not as much as that of curcumin zinc oxide nanoparticles. However, the selectivity index of zinc oxide had general toxicity and showed that it can cause cytotoxicity in normal cells.

The MTT assay results of this study showed that the curcumin zinc oxide nanoparticles were effective against the MCF-7 cell line. The selectivity index of curcumin zinc oxide nanoparticles being greater than 2 indicates that it has selective toxicity toward cancer cells. These findings suggest that the curcumin zinc oxide nanoparticles showed stronger anticancer activity and selectivity toward MCF-7 cancer cells compared to plain curcumin, and by formulating curcumin with zinc oxide nanoparticles, its anticancer potential can be increased along with more selectivity toward cancer cells.

The outcomes of the MTT assay indicated that curcumin zinc oxide nanoparticles exhibit more selectivity in the direction of most cancer cells compared to curcumin or zinc oxide nanoparticles.

**3.3. Genotoxicity (Comet Assay).** The comet assay was used to assess the genotoxicity of different doses of curcumin zinc oxide nanoparticles. Curcumin zinc oxide nanoparticles showed very mild or no DNA damage. Each concentration's damage index was computed and contrasted with the positive control.

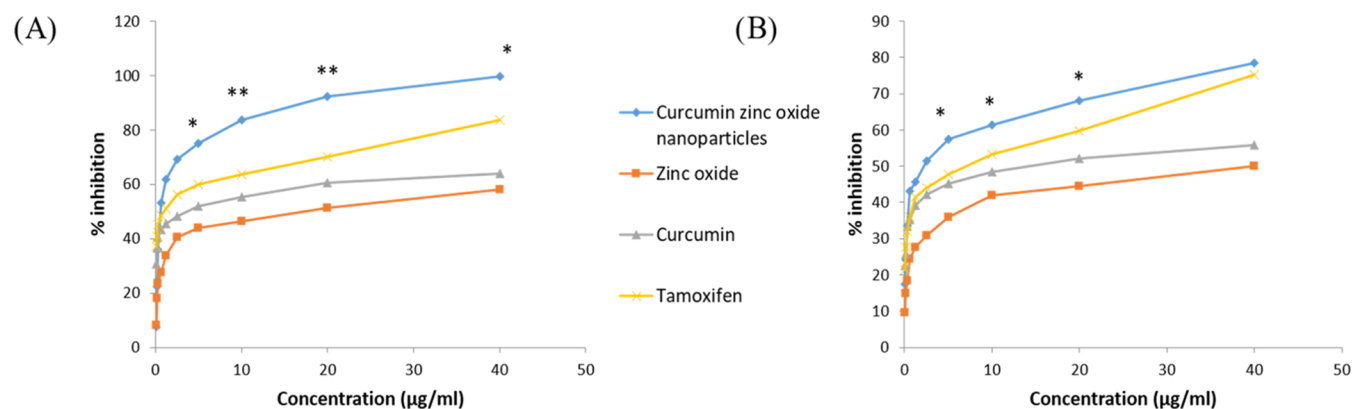


**Figure 4.** Percentage inhibition on MCF-7 and Vero cell lines. The anticancer and cytotoxic potential of curcumin zinc oxide nanoparticles was quantified on MCF-7 (A) and Vero cell lines (B). Ten different concentrations of curcumin zinc oxide nanoparticles were incubated for 48 h with MCF-7 and Vero cell lines. The selectivity index was calculated by IC<sub>50</sub>. Tamoxifen was used as a standard. The data are represented as mean  $\pm$  SEM of 4–5 independent experiments. Comparison is made between curcumin zinc oxide nanoparticles and tamoxifen, where \*  $p < 0.05$  and \*\*  $p < 0.01$ .

The statistically significant results ( $p \leq 0.05$ ) were observed when the comparison was made between negative control and concentrations of each drug. The genetic damage index of curcumin zinc oxide nanoparticles, curcumin, and zinc oxide seen at the highest concentration (40  $\mu\text{g/mL}$ ) was 0.08, 0.12, and 0.28 with fragmentation percentages of 8, 12, and 20%, as given in Tables 2, 3, and 4, respectively. Curcumin zinc oxide nanoparticles produced the least damage to DNA, and no damage was seen at concentrations below 10  $\mu\text{g/mL}$  (Figure 5).

**Table 2. Genetic Damage Index of Different Concentrations of Curcumin Zinc Oxide Nanoparticles<sup>a</sup>**

concentration	damage index	genetic damage index	fragmentation %	mean tail length $n = 25$
40	2	0.08	8	1.26 $\pm$ 0.49**
20	1	0.04	4	1.21 $\pm$ 0.52**
10	1	0.04	4	1.18 $\pm$ 0.65***
5	0	0	0	0.98 $\pm$ 0.83***
2.5	0	0	0	0.96 $\pm$ 0.38***
1.25	0	0	0	0.78 $\pm$ 0.43***
0.625	0	0	0	0.74 $\pm$ 0.56***
0.3125	0	0	0	0.47 $\pm$ 0.43***
0.156	0	0	0	0.38 $\pm$ 0.84***
0.078	0	0	0	0.08 $\pm$ 0.47***
20% DMSO (positive control)	45	1.8	100	5.72 $\pm$ 0.36
normal saline (negative control)	0	0	0	0

<sup>a</sup>The data are shown as mean  $\pm$  SD and representative of 3–5 independent experiments. Comparison is made between positive control and concentrations, where \*  $p < 0.05$ , \*\*  $p < 0.01$ , and \*\*\*  $p < 0.001$ .

**Table 3. Genetic Damage Index of Different Concentrations of Curcumin<sup>a</sup>**

concentration	damage index	genetic damage index	fragmentation %	mean tail length $n = 25$
40	3	0.12	12	1.86 $\pm$ 0.73**
20	2	0.08	8	1.31 $\pm$ 0.74**
10	1	0.04	4	1.28 $\pm$ 0.28***
5	0	0	0	1.14 $\pm$ 0.72***
2.5	0	0	0	0.68 $\pm$ 0.74***
1.25	0	0	0	0.68 $\pm$ 0.35***
0.625	0	0	0	0.54 $\pm$ 0.28***
0.3125	0	0	0	0.57 $\pm$ 0.22***
0.156	0	0	0	0.46 $\pm$ 0.38***
0.078	0	0	0	0.36 $\pm$ 0.47***
20% DMSO (positive control)	45	1.8	100	5.72 $\pm$ 0.27***
normal saline (negative control)	0	0	0	0

<sup>a</sup>The data are shown as mean  $\pm$  SD and representative of 3–5 independent experiments. Comparison is made between positive control and concentrations, where \*  $p < 0.05$ , \*\*  $p < 0.01$ , and \*\*\*  $p < 0.001$ .

It was shown that curcumin zinc oxide nanoparticles produce genotoxicity at higher doses and that comet tails

**Table 4. Genetic Damage Index of Different Concentrations of Zinc Oxide<sup>a</sup>**

concentration	damage index	genetic damage index	fragmentation %	mean tail length $n = 25$
40	7	0.28	20	2.1 $\pm$ 0.57**
20	6	0.24	16	2.46 $\pm$ 0.73*
10	4	0.16	12	1.18 $\pm$ 0.23***
5	1	0.04	4	1.18 $\pm$ 0.84***
2.5	0	0	0	0.46 $\pm$ 0.75***
1.25	0	0	0	0.18 $\pm$ 0.54***
0.625	0	0	0	0.34 $\pm$ 0.53***
0.3125	0	0	0	0.27 $\pm$ 0.22***
0.156	0	0	0	0.08 $\pm$ 0.35***
0.078	0	0	0	0.28 $\pm$ 0.78***
20% DMSO (positive control)	45	1.8	100	5.72 $\pm$ 0.73
normal saline (negative control)	0	0	0	0

<sup>a</sup>The data are shown as mean  $\pm$  SD and representative of 3–5 independent experiments. Comparison is made between positive control and concentrations, where \*  $p < 0.05$ , \*\*  $p < 0.01$ , and \*\*\*  $p < 0.001$ .

may be visible at a concentration of 40  $\mu\text{g/mL}$ . No damage was found within the concentration range of 5–0.078  $\mu\text{g/mL}$ . The mean tail length of the curcumin zinc oxide nanoparticles at the maximum concentration, 40  $\mu\text{g/mL}$ , was 1.26 and was less damaged than the tail length of the positive control (20% DMSO), which was 5.72. No genetic damage index was observed at doses 5  $\mu\text{g/mL}$  to 0.780  $\mu\text{g/mL}$ . The genetic damage index was observed at the very high dose of 40  $\mu\text{g/mL}$ , and it appeared to be 2.

#### 4. DISCUSSION

Pharmaceutical research aimed at improving drug bioavailability, stability, and targeting has advanced significantly. Pharmaceutical nanocarriers are versatile delivery vehicles of submicron size, including polymeric, lipid, and inorganic nanoparticles, liposomes, nanotubes, nanocomplexes, liposomes, and others.<sup>20</sup> In this study, curcumin zinc oxide nanoparticles were synthesized using curcumin and zinc nitrate, which appeared yellow in color. In different studies, Zn oxide nanoparticles have already been studied, and yellow-colored particles have been obtained, as in our study.<sup>21</sup> Nanoparticles of 189 nm size were obtained, and size determination was done by finding the zeta potential of these particles. Some literature describes that the size of nanoparticles below 200 nm is pharmacologically effective, especially for passive targeting of tumors.<sup>22</sup> Research has shown that the nanoparticles of curcumin had a surface charge of  $-35$ , showing good physical and chemical stability of curcumin nanoparticles.<sup>23</sup> UV spectrophotometry is a commonly used and reliable tool for characterizing and quantifying metal nanoparticles in combination with medicinal plants. The UV spectrometry results in our study showed a bend curve, which differentiated the characterization of different metals, like another investigation on the synthesis and characterization of curcumin zinc oxide nanoparticles by UV spectrometry with a bend curve and a peak absorbance at 419 nm.<sup>24</sup> We characterized the ZnO nanoparticle of curcumin, and the results obtained were similar to those

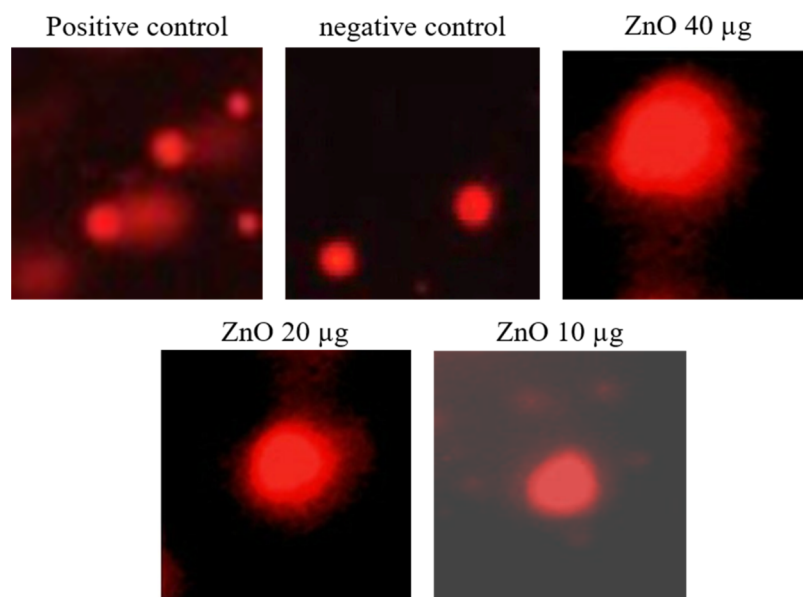


**Figure 5.** Genotoxicity evaluation by the comet assay for curcumin zinc oxide nanoparticles. Freshly isolated human lymphocytes were used for the evaluation of genotoxicity by performing the comet assay. The results are given in the form of representative fluorescence microscopy images of the comet assay for positive control, negative control, and different doses of curcumin zinc oxide nanoparticles.

obtained in previous studies. Research was conducted to assess the shape and size of nanoparticles by using SEM and transmission electron microscopy (TEM). It was interpreted that curcumin zinc oxide nanoparticles were round.<sup>24a</sup> Similar results are found in our research where spherical nanoparticles are obtained. The FTIR after-effects of the current research demonstrate that the arrangement of curcumin zinc oxide nanoparticles was fruitful, and the communications between curcumin and zinc oxide were affirmed. The force and position of the peaks in the FTIR range recommend the chelation of carbonyl or hydroxyl gatherings of curcumin with zinc, which means effective development of the nanocomposite. This sort of examination gives important data about the substance piece and useful gatherings present in the blended nanoparticles, which can help in figuring out their likely applications in different fields, including medication and well-being. The FTIR results showed normal ZnO extending vibrations and fragrant extending vibrations of the benzene ring, as well as the decrease in the force of specific groups, demonstrating the development of a metal–curcumin complex. These outcomes are in concurrence with past examinations utilizing FTIR to describe curcumin zinc oxide nanoparticles.<sup>24a,25</sup> The selectivity index of curcumin zinc oxide is greater than 2, showing that it has selective toxicity toward most cancer cells and can be useful in cancer therapy.<sup>26</sup> This highlights the significance of information about the interactions among the components of the nanocomposite and their impact on biological interest.

We have studied the anticancer and cytotoxic potential of curcumin zinc oxide nanoparticles, and it was quantified on MCF-7 and Vero cell lines, respectively. In our study, we found good anticancer activity with a better selective index. According to recent studies, ZnO nanoparticles (NPs) have been shown to exhibit anticancer properties by inducing the death of cancerous cells and cytotoxicity.<sup>27</sup> The anticancer activity of ZnO NPs on the human breast cancer cell line (MCF-7) showed dose-dependent inhibition, and the IC<sub>50</sub> value was 121  $\mu\text{g}/\text{mL}$  for MCF-7 cells, using tamoxifen (a

commercial chemotherapy drug) as a positive control, which showed the IC<sub>50</sub> value of 8  $\mu\text{g}/\text{mL}$ .<sup>28</sup> Additionally, a study found that when curcumin was combined with zinc oxide NPs, the resulting nanocomposites demonstrated higher cytotoxicity against multiple cancer cell lines, including breast, cervical, osteosarcoma, and myeloma, compared to zinc oxide NPs or curcumin alone.<sup>29</sup> This increased cytotoxicity was attributed to the induction of intracellular reactive oxygen species.

The potential anticancer activity of the synthesized nanocomposites of curcumin with zinc oxide was studied on the rhabdomyosarcoma cell line via the MTT assay, while their cytotoxic effects were tested against human embryonic kidney cells using the resazurin assay. The nanoparticles exhibited the best balance between the two, showing the lowest toxicity against healthy cells and good anticancer activity.<sup>24a</sup> Another study found that nanocomposites of curcumin and zinc oxide had apoptosis effects on MCF7 cells and a better balance between anticancer activity and low toxicity against healthy cells, making them a promising option for cancer therapy.<sup>24b</sup>

These studies comply with the outcomes of this study and imply that curcumin zinc oxide nanoparticles have increased anticancer activity in comparison to curcumin but are slightly less than that of tamoxifen. Additionally, it showcases selective toxicity against cancer cells, making it a promising candidate for further research as an anticancer agent. However, it is important to notice that in vitro studies inclusive of the MTT assay will not reflect the in vivo effects of these medicinal components, and further studies, including animal research and clinical trials, are important to decide their efficacy and safety to be used for cancer treatment. Nanocurcumin was potentially protective against DNA damage induced by tartrazine ingested by rats.<sup>30</sup> Administration of curcumin-silver nanoparticles leads to significant antioxidant activity in vivo and has the potential to prevent DNA damage that results from direct exposure to CCL4.<sup>31</sup> Results obtained from a recent study found that mice treated with curcumin nanoemulsions were effective in reducing DNA damage.<sup>32</sup> Research suggested that the curcumin-loaded Poly(lactic-co-glycolic acid) nanoparticles

can cause a better protective effect than free curcumin against arsenic-induced genotoxicity.<sup>33</sup> Comet assay results confirmed TiO<sub>2</sub> NP-related DNA damage. Remarkably, all of these changes are mitigated in rats treated with curcumin.<sup>34</sup>

## CONCLUSIONS

In conclusion, the prepared curcumin zinc oxide nanoparticles had great potential for anticancer activity with minimum genotoxic effects. These findings are crucial, as the reduced particle size of curcumin zinc oxide nanoparticles is expected to have enhanced cellular uptake, and hence nongenotoxic nature further bolsters their potential as a safe and effective anticancer drug product. To transform these findings into practical applications, additional research is essential. Further studies must be focused on elucidating the underlying mechanisms of the nanoparticles' anticancer action, investigating their long-term effects, and exploring potential combination therapies to enhance their efficacy. Moreover, the development and optimization of efficient dosage forms are vital to maximize the full spectrum of benefits offered by curcumin zinc oxide nanoparticles and minimize any adverse effects.

## ASSOCIATED CONTENT

### Supporting Information

The Supporting Information is available free of charge at <https://pubs.acs.org/doi/10.1021/acsomega.4c01489>.

Images of SEM analysis of curcumin zinc oxide nanoparticles on different magnifications (PDF)

## AUTHOR INFORMATION

### Corresponding Author

Muhammad Ovais Omer – Department of Pharmacology and Toxicology, University of Veterinary and Animal Sciences, Lahore 54000, Pakistan; Phone: +924299211449; Email: [drovaisomer@uvas.edu.pk](mailto:drovaisomer@uvas.edu.pk)

### Authors

Alia Saif – Department of Pharmacology and Toxicology, University of Veterinary and Animal Sciences, Lahore 54000, Pakistan; [orcid.org/0000-0002-9172-5802](https://orcid.org/0000-0002-9172-5802)

Adeel Sattar – Department of Pharmacology and Toxicology, University of Veterinary and Animal Sciences, Lahore 54000, Pakistan

Yasin Tipu – Department of Pathology, University of Veterinary and Animal Sciences, Lahore 54000, Pakistan

Hanan M. Alharbi – Department of Pharmaceutics, College of Pharmacy, Umm Al-Qura University, Makkah 21955, Saudi Arabia; [orcid.org/0000-0001-8393-8931](https://orcid.org/0000-0001-8393-8931)

Uzma Saher – Department of Pharmacy, The Women University, Multan 60000, Pakistan; [orcid.org/0000-0002-3519-7873](https://orcid.org/0000-0002-3519-7873)

Tanzeela Awan – Bakhtawar Amin College of Pharmaceutical Sciences, Multan 60000, Pakistan

Complete contact information is available at:

<https://pubs.acs.org/doi/10.1021/acsomega.4c01489>

### Author Contributions

A.S.: conceptualization and methodology, investigation, and writing—original draft and review and editing. M.O.O.: supervision, conceptualization and methodology, and review—original draft. A.S.: result finalization and review—original draft. Y.T.: review—original draft. H.M.A.: review—

original draft and proofreading. U.S.: review—original draft and grammar checking. T.A.: review—original draft and statistical analysis

### Notes

The authors declare no competing financial interest.

## ACKNOWLEDGMENTS

The authors would like to thank the services given by Dr. Arifa Saif and the staff of the Department of Pharmacology & Toxicology, University of Veterinary & Animal Sciences, Lahore, Pakistan, for their kind assistance in conducting the research.

## ABBREVIATIONS

UV-spectrophotometer	UV-visible spectrophotometer
SEM	scanning electron microscopy
FTIR	Fourier transform infrared
MTT assay	3-(4,5-dimethylthiazol-2-yl)-2,5-diphenyl-2H-tetrazolium bromide
DNA	deoxyribonucleic acid
ZnO	zinc oxide
NaOH	sodium hydroxide
NADPH	nicotinamide adenine dinucleotide phosphate
TEM	transmission electron microscopy
CCL4	carbon tetrachloride

## REFERENCES

- (1) (a) Giaquinto, A. N.; Miller, K. D.; Tossas, K. Y.; Winn, R. A.; Jemal, A.; Siegel, R. L. Cancer statistics for African American/Black People 2022. *Ca-Cancer J. Clin.* **2022**, *72* (3), 202–229. (b) Miller, K. D.; Ortiz, A. P.; Pinheiro, P. S.; Bandi, P.; Minihan, A.; Fuchs, H. E.; Martinez Tyson, D.; Tortolero-Luna, G.; Fedewa, S. A.; Jemal, A. M.; Siegel, R. L. Cancer statistics for the US Hispanic/Latino population, 2021. *Ca-Cancer J. Clin.* **2021**, *71* (6), 466–487. (c) Milosevic, M.; Jankovic, D.; Milenkovic, A.; Stojanov, D. Early diagnosis and detection of breast cancer. *Technol. Health Care* **2018**, *26* (4), 729–759.
- (2) Pudkasam, S.; Tangalakis, K.; Chinlumprasert, N.; Apostolopoulos, V.; Stojanovska, L. Breast cancer and exercise: The role of adiposity and immune markers. *Maturitas* **2017**, *105*, 16–22.
- (3) Hoang, A. T. N.; Hoe, K.-L.; Lee, S.-J. CSNK1G2 differently sensitizes tamoxifen-induced decrease in PI3K/AKT/mTOR/S6K and ERK signaling according to the estrogen receptor existence in breast cancer cells. *PLoS One* **2021**, *16* (4), No. e0246264, DOI: [10.1371/journal.pone.0246264](https://doi.org/10.1371/journal.pone.0246264).
- (4) Wink, M. Modes of action of herbal medicines and plant secondary metabolites. *Medicines* **2015**, *2* (3), 251–286.
- (5) Ugboko, H. U.; Nwinyi, O. C.; Oranus, S. U.; Fatoki, T. H.; Omonhinmin, C. A. Antimicrobial Importance of Medicinal Plants in Nigeria. *Sci. World J.* **2020**, *2020*, No. 7059323.
- (6) Damyeh, M. S.; Mereddy, R.; Netzel, M. E.; Sultanbawa, Y. An insight into curcumin-based photosensitization as a promising and green food preservation technology. *Compr. Rev. Food Sci. Food Saf.* **2020**, *19* (4), 1727–1759, DOI: [10.1111/1541-4337.12583](https://doi.org/10.1111/1541-4337.12583).
- (7) Arlı, M.; Çelik, H. The Biological Importance of Curcumin. *East Anatolian J. Sci.* **2020**, *6*, 21–34.
- (8) Anand, P.; Kunnumakkara, A. B.; Newman, R. A.; Aggarwal, B. B. Bioavailability of curcumin: problems and promises. *Mol. Pharmaceutics* **2007**, *4* (6), 807–818.
- (9) Gupta, S. C.; Patchva, S.; Aggarwal, B. B. Therapeutic roles of curcumin: lessons learned from clinical trials. *AAPS J.* **2013**, *15* (1), 195–218.
- (10) Parveen, K.; Banse, V.; Ledwani, L. In *Green Synthesis of Nanoparticles: Their Advantages and Disadvantage*, AIP Conference Proceedings; AIP Publishing LLC, 2016.



- (11) Liu, S.; Yu, B.; Wang, S.; Shen, Y.; Cong, H. Preparation, surface functionalization and application of Fe<sub>3</sub>O<sub>4</sub> magnetic nanoparticles. *Adv. Colloid Interface Sci.* **2020**, *281*, No. 102165.
- (12) Gour, A.; Jain, N. K. Advances in green synthesis of nanoparticles. *Artif. Cells, Nanomed., Biotechnol.* **2019**, *47* (1), 844–851.
- (13) Perera, W. P. T. D.; Dissanayake, R. K.; Ranatunga, U.; Hettiarachchi, N.; Perera, K.; Unagolla, J. M.; De Silva, R.; Pahalagedara, L. Curcumin loaded zinc oxide nanoparticles for activity-enhanced antibacterial and anticancer applications. *RSC Adv.* **2020**, *10* (51), 30785–30795.
- (14) Kamshad, M.; Talab, M. J.; Beigoli, S.; Sharifirad, A.; Chamani, J. Use of spectroscopic and zeta potential techniques to study the interaction between lysozyme and curcumin in the presence of silver nanoparticles at different sizes. *J. Biomol. Struct. Dyn.* **2019**, *37* (8), 2030–2040, DOI: 10.1080/07391102.2018.1475258.
- (15) Saravanakumar, A.; Peng, M. M.; Ganesh, M.; Jayaprakash, J.; Mohankumar, M.; Jang, H. T. Low-cost and eco-friendly green synthesis of silver nanoparticles using *Prunus japonica* (Rosaceae) leaf extract and their antibacterial, antioxidant properties. *Artif. Cells, Nanomed., Biotechnol.* **2017**, *45* (6), 1165–1171.
- (16) Dara, M.; Hassanpour, M.; Amiri, O.; Baladi, M.; Salavati-Niasari, M. Tb<sub>2</sub>CoMnO<sub>6</sub> double perovskites nanoparticles as photocatalyst for the degradation of organic dyes: Synthesis and characterization. *Arabian J. Chem.* **2021**, *14* (10), No. 103349.
- (17) Aziz, A.; Ali, N.; Khan, A.; Bilal, M.; Malik, S.; Ali, N.; Khan, H. Chitosan-zinc sulfide nanoparticles, characterization and their photocatalytic degradation efficiency for azo dyes. *Int. J. Biol. Macromol.* **2020**, *153*, 502–512, DOI: 10.1016/j.ijbiomac.2020.02.310.
- (18) Hartmann, A.; Agurell, E.; Beevers, C.; Brendler-Schwaab, S.; Burlinson, B.; Clay, P.; Collins, A.; Smith, A.; Speit, G.; Thybaud, V. Recommendations for conducting the in vivo alkaline Comet assay. *Mutagenesis* **2003**, *18* (1), 45–51.
- (19) (a) Clarke, S. Development of Hierarchical Magnetic Nanocomposite Materials for Biomedical Applications. Ph.D. Thesis, Dublin City University, 2013. (b) Danaei, M.; Dehghankhold, M.; Ataei, S.; Davarani, F. H.; Javanmard, R.; Dokhani, A.; Khorasani, S.; Mozafari, M. J. P. Impact of particle size and polydispersity index on the clinical applications of lipidic nanocarrier systems. *Pharmaceutics* **2018**, *10* (2), No. 57, DOI: 10.3390/pharmaceutics10020057.
- (20) Alshawwa, S. Z.; Kassem, A. A.; Farid, R. M.; Mostafa, S. K.; Labib, G. S. J. P. Nanocarrier Drug Delivery Systems: Characterization, Limitations, Future Perspectives and Implementation of Artificial Intelligence. *Pharmaceutics* **2022**, *14* (4), No. 883, DOI: 10.3390/pharmaceutics14040883.
- (21) Patra, D.; El Kurdi, R. Curcumin as a novel reducing and stabilizing agent for the green synthesis of metallic nanoparticles. *Green Chem. Lett. Rev.* **2021**, *14* (3), 474–487.
- (22) Maeda, H. Toward a full understanding of the EPR effect in primary and metastatic tumors as well as issues related to its heterogeneity. *Adv. Drug Delivery Rev.* **2015**, *91*, 3–6, DOI: 10.1016/j.addr.2015.01.002.
- (23) Abu-Taweel, G. M.; Attia, M. F.; Hussein, J.; Mekawi, E. M.; Galal, H. M.; Ahmed, E. I.; Allam, A. A.; El-Naggar, M. E. J. B. Pharmacotherapy, Curcumin nanoparticles have potential antioxidant effect and restore tetrahydrobiopterin levels in experimental diabetes. *Biomed. Pharmacother.* **2020**, *131*, No. 110688, DOI: 10.1016/j.biopha.2020.110688.
- (24) (a) Perera, W.; Dissanayake, R. K.; Ranatunga, U.; Hettiarachchi, N.; Perera, K.; Unagolla, J. M.; De Silva, R. T.; Pahalagedara, L. R. Curcumin loaded zinc oxide nanoparticles for activity-enhanced antibacterial and anticancer applications. *RSC Adv.* **2020**, *10* (51), 30785–30795, DOI: 10.1039/D0RA05755J. (b) Sawant, V.; Bamane, S. R. PEG-beta-cyclodextrin functionalized zinc oxide nanoparticles show cell imaging with high drug payload and sustained pH responsive delivery of curcumin in to MCF-7 cells. *J. Drug Delivery Sci. Technol.* **2018**, *43*, 397–408, DOI: 10.1016/j.jddst.2017.11.010.
- (25) Kumar, H.; Rani, R. Structural and optical characterization of ZnO nanoparticles synthesized by microemulsion route. *Int. Lett. Chem., Phys. Astron.* **2013**, *14*, 26–36, DOI: 10.56431/p-q38442.
- (26) Singh, K.; Gangrade, A.; Jana, A.; Mandal, B. B.; Das, N. Design, Synthesis, Characterization, and Antiproliferative Activity of Organoplatinum Compounds Bearing a 1,2,3-Triazole Ring. *ACS Omega* **2019**, *4* (1), 835–841.
- (27) (a) Taccola, L.; Raffa, V.; Riggio, C.; Vittorio, O.; Iorio, M. C.; Vanacore, R.; Pietrabissa, A.; Cuschieri, A. Zinc oxide nanoparticles as selective killers of proliferating cells. *Int. J. Nanomed.* **2011**, *6*, 1129–1140, DOI: 10.2147/ijn.s16581. (b) Ostrovsky, S.; Kazimirsky, G.; Gedanken, A.; Brodie, C. Selective cytotoxic effect of ZnO nanoparticles on glioma cells. *Nano Res.* **2009**, *2* (11), 882–890, DOI: 10.1007/s12274-009-9089-5.
- (28) Moghaddam, A. B.; Moniri, M.; Azizi, S.; Rahim, R. A.; Ariff, A. B.; Navaderi, M.; Mohamad, R. Eco-Friendly Formulated Zinc Oxide Nanoparticles: Induction of Cell Cycle Arrest and Apoptosis in the MCF-7 Cancer Cell Line. *Genes* **2017**, *8* (10), No. 281, DOI: 10.3390/genes8100281.
- (29) Somu, P.; Paul, S. A biomolecule-assisted one-pot synthesis of zinc oxide nanoparticles and its bioconjugate with curcumin for potential multifaceted therapeutic applications. *New J. Chem.* **2019**, *43* (30), 11934–11948, DOI: 10.1039/C9NJ02501D.
- (30) El-Desoky, G. E.; Wabaidur, S. M.; AlOthman, Z. A.; Habila, M. A. Regulatory role of nano-curcumin against tartrazine-induced oxidative stress, apoptosis-related genes expression, and genotoxicity in rats. *Molecules* **2020**, *25* (24), No. 5801, DOI: 10.3390/molecules25245801.
- (31) Ebaid, H.; Habila, M.; Hassan, I.; Al-Tamimi, J.; Omar, M. S.; Rady, A.; Alhazza, I. M. Curcumin-containing Silver Nanoparticles Prevent Carbon Tetrachloride-induced Hepatotoxicity in Mice. *Comb. Chem. High Throughput Screening* **2021**, *24* (10), 1609–1617, DOI: 10.2174/1386207323666201211100830.
- (32) Abdelmoneam, E.; Rageh, M.; Mohamad, E. Antitumor efficacy of Curcumin nanoparticles. *Egypt. J. Chem.* **2022**, *66*, 403–406, DOI: 10.21608/ejchem.2022.152966.6623.
- (33) Sankar, P.; Telang, A. G.; Ramya, K.; Vijayakaran, K.; Kesavan, M.; Sarkar, S. N. Protective action of curcumin and nano-curcumin against arsenic-induced genotoxicity in rats in vivo. *Mol. Biol. Rep.* **2014**, *41*, 7413–7422, DOI: 10.1007/s11033-014-3629-0.
- (34) El-Din, E. A. A.; Mostafa, H. E.-S.; Samak, M. A.; Mohamed, E. M.; El-Shafei, D. Could curcumin ameliorate titanium dioxide nanoparticles effect on the heart? A histopathological, immunohistochemical, and genotoxic study. *Environ. Sci. Pollut. Res.* **2019**, *26*, 21556–21564, DOI: 10.1007/s11356-019-05433-2.